SYNTHESIS AND CHARACTERIZATION OF NOVEL BIOPLASTICS BY ADVANCED MANUFACTURING TECHNIQUES

by

Saud Ali Abu Aldam

Bachelor of Science, University of North Dakota, 2018

A Thesis

Submitted to the Graduate Facility

of the

University of North Dakota

In partial fulfillment of the requirements

For the degree of

Master of Science

Grand Forks, North Dakota

December

2019

This thesis, submitted by Saud Ali Abu Aldam in partial fulfillment of the requirements for the Degree of Master of Science in Mechanical Engineering from the University of North Dakota, has been read by the Faculty Advisory Committee under whom the work has been done and is hereby approved.
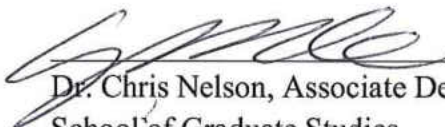
_____
Dr. Surojit Gupta

_____
Dr. Yun Ji

_____
Dr. Clement Tang

This thesis is being submitted by the appointed advisory committee as having met all of the requirements of the School of Graduate Studies at the University of North Dakota and is hereby approved.

_____
Dr. Chris Nelson, Associate Dean
School of Graduate Studies

12/16/19
_____
Date

PERMISSION

Title   Synthesis and Characterization of Novel Bioplastics by Advanced Manufacturing
      Techniques

Department Mechanical Engineering

Degree   Master of Science

   In presenting this thesis in fulfillment of the requirements for a graduate degree from the University of North Dakota, I agree that the library of this University shall make it freely available for inspection. I further agree that permission for extensive copying for scholarly purposes may be granted by the professor who supervised my thesis work or, in his absence, by the chairperson of the department or the dean of the School of Graduate Studies. It is understood that any copying or publication or other use of this thesis or part thereof for financial gain shall not be allowed without my written permission. It is also understood that due recognition shall be given to me and to the University of North Dakota in any scholarly use which may be made of any material in my thesis.

Saud Abu Aldam
12.05.2019

TABLE OF CONTENTS

LIST OF FIGURES

LIST OF TABLES

ACKNOWLEDGMENTS

During my Master's degree journey, there are many people and organizations that supported me throughout this memorable experience.

First, I wish to acknowledge the guidance and support from my advisor Dr. Gupta. Thank you very much for everything.

I would like to thank all my colleagues in the advanced materials research group for the good times we spent in and out the laboratory.

I want to thank the Saudi Arabian Cultural Mission to the US (SACM), ND Venture Grant, and Dean Professorship for funding.

Last but not least, I want to thank my family and friends, especially my parents Ali and Laila, my sister Nadyah, and my friend Kevin Robertson.

ABSTRACT

This thesis reports the synthesis and characterization of novel bioplastics by using solvent casting as a fabrication method. Literature survey suggests that having a sustainable economy is of great importance for today people and generations to come. It is expected that biodegradable and biocompatible plastics such as Polylactic Acid (PLA), Polyhydroxyalkanoates (PHAs), and Cellulose Acetate (CA) will assist in achieving green and eco-friendly environment. Chapter I summarizes background information about PLA, PHAs, and CA. Chapter II summarizes the synthesis and characterization of the materials outlined in Chapter I. Chapters III documents the integration of lignin and micro-sliver particulates as additives in PLA-PHA matrix. Finally, conclusions and future work will be summarized.

CHAPTER I

INTRODUCTION

1.1 Introduction

1.1.1 Plastic and Sustainable Economy

Circular economy has emerged as an important component of sustainable economic development [1]. Fundamental research on plastics from the perspective of circular economy and sustainability has become important for our current generation [2]. Ellen MacArthur Foundation has envisioned New Plastics Economy based around the principles of circular economy which will use plastics from renewable sources and will strive to eliminate the deleterious effect of plastic usage on environment [3].

Plastics derived from renewable sources are referred to as bioplastics [4]. A sub-category of bioplastics is biodegradable. Some of the examples of biodegradable bioplastics are cellulose (e.g. cellulose acetate and cellulose xanthate/cellophane), Poly Lactic Acid (PLA), and Polyhydroxyalkaonate (PHA). These bioplastics are especially important from environmental perspective [4-10].

1.1.2 Polylactic Acid

Polylactic Acid (PLA) is a renewable aliphatic polyester which is completely synthesized from renewable resources such as corn starch [5-7]. PLA is commonly synthesized by ring-opening polymerization of the cyclic lactide dimer [7]. Environmental degradation of PLA can take place by a two-step process where, (a) high molecular weight polyester chains are hydrolyzed into lower molecular weight oligomers, (b) and then these oligomers are degraded into water, CO_2, and humus [7]. PLA is also non-toxic, biocompatible, and biodegradable [4, 5]. Some of the

properties of PLA are; glass transition temperature (T_g) (55-60 $_oC$), melting point (T_m) (145-160 $_oC$, and tensile strength of 60 MPa [8].

1.1.3 Polyhydroxyalkanoates

Polyhydroxyalkanoates (PHAs) are polyesters of different hydroalkaonates [9, 10]. PHA is also derived from renewable sources. Reddy at al. [9] have reported that at least 75 different genera of gram-positive and gram-negative bacteria can synthesize PHA. These biodegradable polymers are deposited inside the cells. Due to intricate diversity of the process, multiple types of PHA with engineered molecular mass between 50,000 to 1,000,000 Da and tailored properties can be designed. PHA is also non-toxic, biocompatible, and biodegradable thermoplastics with high degree of crystallinity and polymerization [9]. PHAs have many practical applications including packing films, shampoo bottles, plastic bags, razors, feminine hygiene products, medical surgical garments, carpets and upholstery [9, 10].

1.1.4 Cellulose Acetate

Lignocellulose based bioplastics have also attracted a lot of attention for designing decomposable bioplastics [4, 11, 12]. Cellulose is a linear polysaccharide which constitutes 35-50% of plant cell wall whereas rest of the plant matter is lignin and hemicellulose. It is used for food packaging, coatings, and other relevant industrial applications [11]. Different types of derivatives of cellulose, for example cellulose acetate, have been studied to overcome the limited solubility of cellulose in organic solvents [12, 13]. Cellulose acetate (CA) is obtained by reacting cellulose with acetic anhydride and acetic acid in the presence of sulfuric acid. The solubility of CA is dependent on degree of substitution (DS) of the acetate group. The most common version of CA which is also referred to "acetate" has approximately 2–2.5 acetate group of every three hydroxyls. DS also governs the solubility of cellulose acetate and the solubility of CA can be tailored by DS. It is well documented CA with DS of 2-2.5 is soluble in acetone, dioxane, and

methyl acetate, and higher converted fractions are soluble in dichloromethane [13]. CA is also bestowed with excellent properties like biodegradability, biocompatibility, and insolubility in water which makes it a potential candidate material for membranes, nanocomposites, biomedical applications, among others [12, 13].

Currently, only 9% of conventional plastic is recycled, 12% is incinerated, and 79% is thrown away in landfills, or allowed to litter in environment. It is also predicted that 12,000 metric tons will go into landfills or natural environment by 2050 [14]. Based on 2015 and 2016 data, the share of bioplastic is less than 1% [15, 16]. Clearly, further research in design engineering of bioplastics is important for increasing the popularity and market share of biodegradable and renewable plastics.

Various researchers have tried to optimize the bio-based polymers by forming blends and/or composites [17, 18]. For example, poor formability of poly(hydroxybutyrate) (PHB) (simple and common representative of PHA) has the potential to be improved by adding PLA [17]. Nanofillers like cellulose, nanoclays, Carbon nanotubes, graphene can also tailor the properties of bio-based polymers for a specific application [18]. However, from fundamental perspective if the blend can be designed by composition engineering, then the engineered blend can be used as a matrix for fabricating composites.

The aim of Chapter II is to understand the mechanical and thermal behavior of binary blends (PLA-PHA, PLA-CA, PHA-CA), and ternary blend (PLA-PHA-CA) by systematically engineering the volume fraction of different constituents in the blends. In addition, the morphology study for the all designed compositions will be discussed. The content of Chapters I and II are to be submitted for publication in the Journal of Materials Engineering and Performance. Chapter III will discuss the design of novel PLA-PHA composites by using lignin and micro-silver particulates

as additives. The thermal and the mechanical behaviors will be reported. At the end of Chapter III,

conclusions and future work will be stated.

CHAPTER II

ON THE SYNTHESIS AND CHARACTERIZATION OF POLY LACTIC ACID (PLA), POLYHYDROXYALKANOATE (PHA), CELLULOSE ACETATE (CA), AND THEIR ENGINEERED BLENDS BY SOLVENT CASTING

2.1 Experimental Details

2.1.1 Fabrication of PLA, PHA, and PLA-PHA Blends

Solvent casting was used to manufacture all compositions. Figure 2.1 shows the schematics of the entire process. During the manufacturing process, granules of PLA (4043D PLA Pellets, Filabot, Barre, VT (MW of 110,000-115,000 g/mol [19-20]) and/or PHA (Polyhydroxyalkaonate – Biopolymer (PHA) Granule, Goodfellow, Coraopolis, PA) were used a precursor. Table 2.1 summarizes different types of PHA-PLA blends fabricated during this study. For fabricating PHA compositions, calculated amount of PHA pellets and DCM (Dichloromethane, anhydrous, $\geq$ 99.9%, Sigma-Aldrich, St. Louis, MO) were poured in a sealable glass jar (Sure Tight, Kerr, Atlanta, GA). The mixture was then stirred (Magnetic Stirrer model: SH-2, Huanghua Faithful Instrument Co., Ltd, Huanghua City, China) for 2 h by using a Teflon coated magnetic stirrer until PHA was completely dissolved in DCM. From the DCM-PHA solution, ~8 g of solution was poured into each compartment of Teflon coated pan (12-Cavity Muffin Pan Stock No. 2105-4960, Wilton, Naperville, IL) to produce at least 5 samples. The solvent cast samples were then cured in the ambient environment for 24 h. The sample was demolded and then cut into coupons for tensile testing by a scissor. Finally, the coupons were dried in a furnace (DZF-Series, MTI Corporation, Richmond, CA) at 100 ₀C for 24 h to completely remove DCM from the coupons. Films of PLA and different blends of PLA-PHA were also fabricated by the same procedure. By using the density of PLA and PHA as 1.24 g/cc and 1.23 g/cc, respectively, the results are also reported in volume fractions.

Table 2.1: List of fabricated samples for PLA-PHA compositions

Composition (vol%)	PLA (g)	PHA (g)	PLA‡ (Vol Fraction (%))	PHA‡ (Vol Fraction (%))
100 PHA	N/A	5	0	100
100 PLA	5	N/A	100	0
50 PLA – 50 PHA	2.25	2.25	50	50
75 PLA - 25PHA	3.75	1.25	75	25
25 PLA - 75 PHA	1.25	3.75	25	75

‡Rounded to near decimal place

2.1.2 Fabrication of Cellulose Acetate by Solvent Casting Method

Cellulose Acetate (CA) based samples were also fabricated by solvent casting. For fabricating CA samples, 5 g of Cellulose Acetate (Cellulose Acetate average Mn ~ 30,000 by GPC, Sigma-Aldrich, St. Louis, MO) and 50 mL of acetone (Acetone for HPLC, ≥ 99.9%, Sigma-Aldrich, St. Louis, MO) were placed in a glass jar (Clear Tall Straight Sided Jars, VWR Corp. #8, Suwanee, GA). The jar was then placed on a magnetic stir plate with Teflon coated stirrers and mixed at room temperature for 2 h until CA was completely dissolved in acetone. Thereafter, 8 g of the mixture was poured into individual compartment of a Teflon coated pan. The castes samples were cured for 24 h in ambient air, and then demolded. The samples were trimmed to obtain a dog-bone coupon for mechanical testing by using scissors. Finally, the tensile coupons were dried in the furnace at 100 oC for 24 hours.

2.1.3 Fabrication of CA-PLA, CA-PHA, and ternary blend CA-PLA-PHA Blends by Solvent Mixing Method

The fabrication procedure for CA-PLA, CA-PHA, and CA-PLA-PHA blends were similar. They were fabricated by solvent mixing and subsequent casting. For example, 49 CA – 51 PHA

composition was fabricated by the following procedure. Initially, PHA and CA solutions were fabricated by the procedure described in Sections 2.1.1 and 2.1.2, respectively. Thereafter, 15 mL of CA and PHA solution were poured separately in a graduated measuring glass cylinder. The solution was then poured in a sealable glass jar. The resultant mixture was mixed for 5 min by magnetic stirring in the glass jar. Thereafter, 8 g of resultant mixture was poured in Teflon coated pan and dried in ambient air for 24 h. The resultant partially dried samples were then cut for tensile testing coupons by a scissor. The coupons were then completely dried by heating at 100 $_o$C for 24 h in the furnace. Table 2.2 shows the summary of designed compositions characterized during this study.
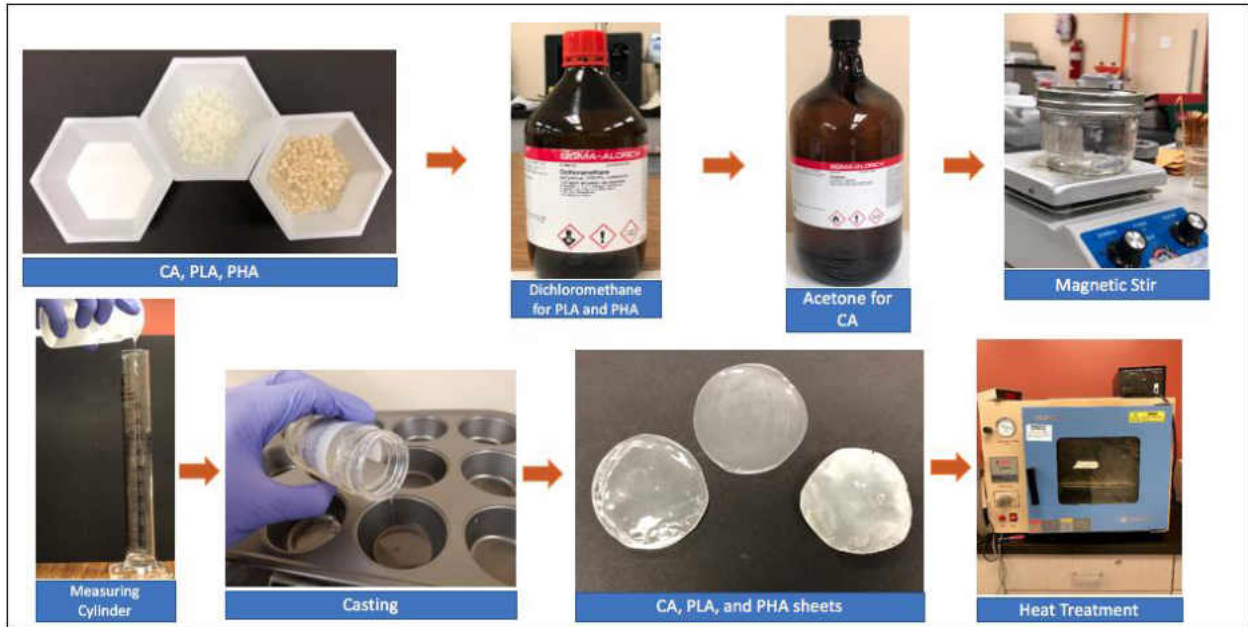
Figure 2.1: Overview of fabrication method for PLA-PHA and Cellulose Acetate composites.

Table 2.2: List of fabricated samples for CA-PHA, CA-PLA, and CA-PLA-PHA composites

Composition (vol%)‡	CA-Acetone Solution (mL)	PLA-DCM Solution (mL)	PHA-DCM Solution (mL)
89.5 CA - 10.5 PHA	27	N/A	3

74 CA - 26 PHA	22.5	N/A	7.5
49 CA - 51 PHA	15	N/A	15
24 CA - 76 PHA	7.5	N/A	22.5
74 CA - 26 PLA	22.5	7.5	N/A
24 CA - 76 PLA	7.5	22.5	N/A
49 CA - 51 PLA	15	15	N/A
5 CA - 47 PLA - 48 PHA	1.5	14.25	14.25
19 CA – 40 PLA - 41 PHA	6	12	12
32 CA - 34 PLA - 34 PHA	9.9	9.9	10.2
59 CA - 20 PLA - 21 PHA	18	6	6
79 CA - 10.5 PLA - 10.5 PHA	24	3	3

‡Rounded to near decimal place; density of CA = 1.3 g/cc

2.1.4 Materials Characterization

2.1.4.1 Mechanical Testing

Figure 2.2 shows the schematics of dog bone sample used for tensile testing. After the drying process, PLA, PHA, CA, and their blends were tested by using a mechanical testing unit (Shimadzu AD-IS UTM, Shimadzu Scientific Instruments Inc., Columbia, MD) at a deflection rate of 5 mm/min by using a load cell of 5 kN. Before conducting the tensile test, the width and thickness of the samples were measured for three times by using a using a Vernier Caliper. The gauge area was calculated from the measured thickness and width of the samples. Due to testing constraints, a typical tensile stress versus displacement plot will be reported instead of stress versus strain plot. The maximum stress at which a sample failed is referred to as Ultimate Tensile Strength (UTS) in the text.

2.1.4.2 Thermal Analysis of the Blends

Thermal behavior of the blends was studied by Differential Scanning Calorimetry (DSC Q1000, TA Instruments, New Castle, DE 19720). During DSC of PLA, PHA, or their

blends, a few mg of samples were heated at 20 oC/min from RT to 200 oC (first cycle) then cooled

to room temperature (RT), thereafter they were again heated at 20 oC/min to 200 oC (second cycle).

The DSC results are reported for both the first and second cycle. During analysis of CA based

compositions, the data was collected when the samples were heated at 20 oC/min from RT to ~260

oC. The results during this reheating cycle is reported in the manuscript.
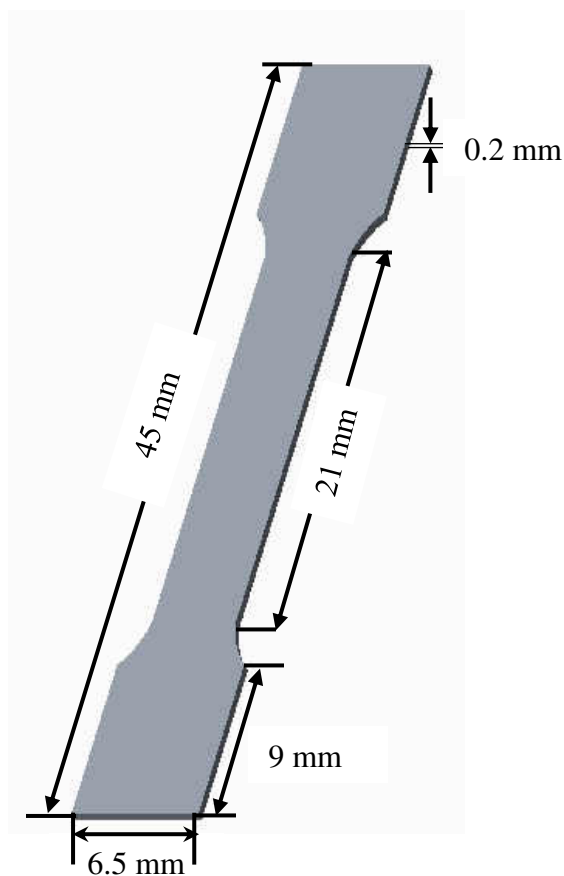
Figure 2.2: Schematics of dog bone sample used for tensile testing.

2.1.4.3 Microstructure Analysis

Digital camera in a smartphone (iPhone 8 Plus 256GB Gold, Apple, Cupertino, CA) was

used to take pictures of all the solvent cast samples. For electron microscopy, all the samples were

polished until ~1 µm finishing. The SE (Secondary Electron) and BSE (Back Scattered Electron)

9

images of the microstructure of polished samples were obtained by using a JEOL JSM-6490LV Scanning Electron Microscope (JEOL USA, Inc., Peabody, Massachusetts) after mounting the polished samples on Al mounts after coating them with Au/Pd (Balzers SCD 030 sputter coater , BAL-TEC RMC, Tucson, AZ). In addition, the Au/Pd coated fractured surface of different blends were also evaluated after tensile testing.

2.2 Results and Discussion

2.2.1 Analysis of Microstructure

Figure 2.3 shows the digital pictures of different solvent cast samples. The solvent cast PLA looked uniform (Fig. 2.3a) whereas PHA (Fig. 2.3b) and CA (Fig. 2.3c) showed visible defects like wrinkling which may be due to evaporation of solvent during casting. The solvent cast blend of 50 PLA – 50 PHA showed signs inhomogeneity which may be indicative of phase separation (Fig. 2.3d). The signs of phase separation in CA-PLA blends were adverse. 24 CA – 76 PLA (Fig. 2.3e) and 49 CA – 51 PLA (Fig. 2.3f) showed visible signs of demixing. The PLA and CA rich regions completely separated in 74 CA – 26 PLA (Fig. 2.3g). Due to this reason, the mechanical behavior of 74 CA – 26 PLA is not reported in this paper as the cast sample could not be machined. Comparatively, the CA-PHA blends (Figs. 2.3 h-k), and CA-PHA-PLA (Figs. 2.3 l-o) showed relative uniform surface but visible signs of defect like pin-holes (Fig. 2.3i), and warping (Figs. 2.3m-n) were observed.
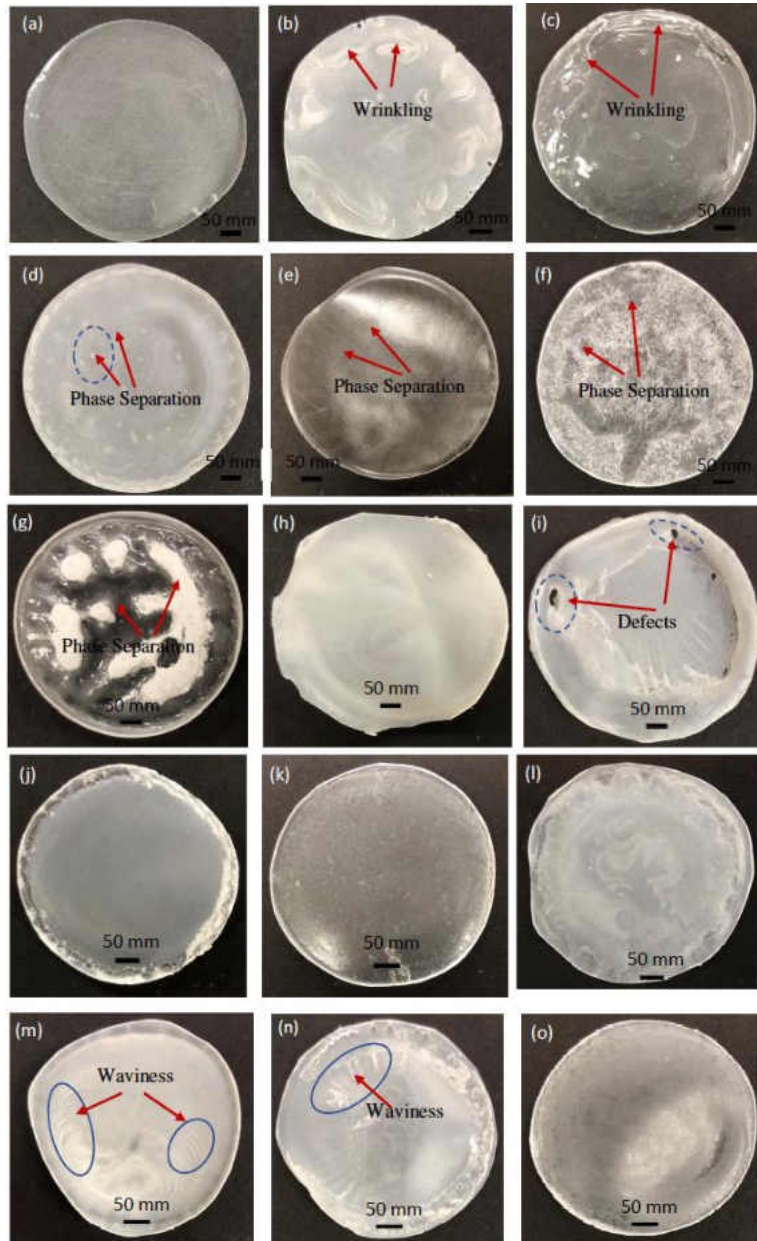
Figure 2.3: Digital pictures of, (a) PLA, (b) PHA, (c) CA, (d) 50 PLA – 50 PHA, (e) 24 CA – 76 PLA, (f) 49 CA – 51 PLA, (g) 74 CA – 26 PLA, (h) 24 CA – 76 PHA, (i) 49 CA – 51 PHA, (j) 74 CA – 26 PHA, (k) 89.5 CA – 10.5 PHA, (l) 5 CA – 47 PLA – 48 PHA, (m) 19 CA – 40 PLA – 41 PHA, (n) 32 CA – 34 PHA – 34 PLA, and (o) 79 CA – 10.5 PHA – 10.5 PLA.

Figure 2.4 shows the SEM micrographs of solvent casted PLA, PHA, and CA samples. PLA sample showed smooth surface (Fig. 2.4a), whereas PHA (Fig. 2.4b) and CA (Fig. 2.4c) showed signs of surface waviness and ridges. These features may be caused by the evaporation of solvent during the solvent casting process. Comparatively, Figure 2.5 shows the microstructure of PHA-PLA blends. In general, the 75 PLA – 25 PHA surface (Fig. 2.5a) looked uniform but microscopic features like waviness became more discernible as the PHA content was increased in the composite system (Figs. 2.5b and 2.5c).
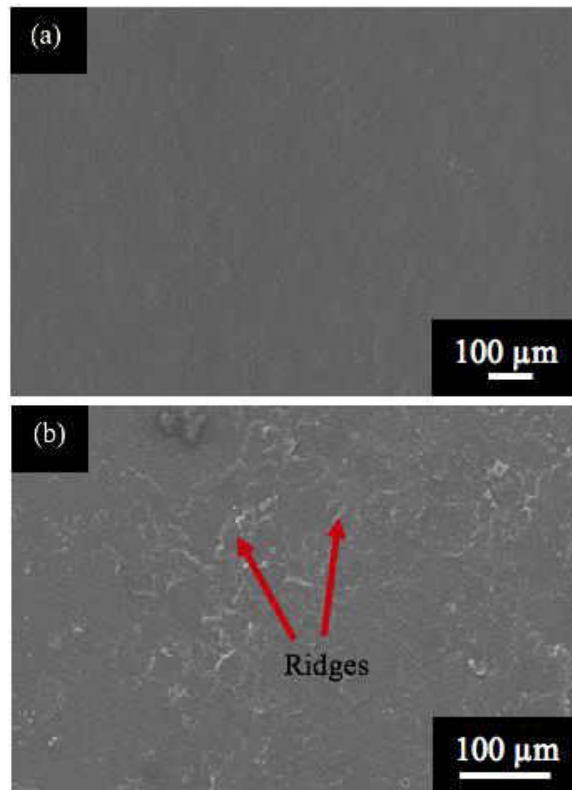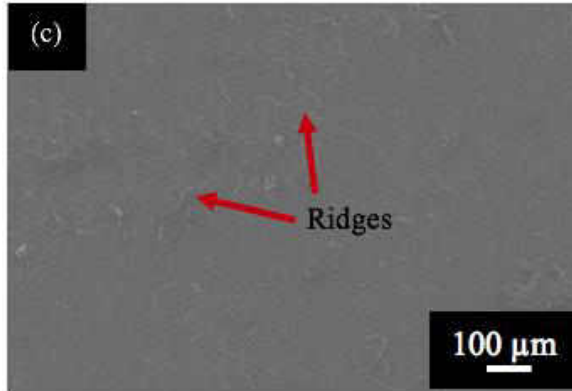
Figure 2.4: SE SEM micrographs of polished surface of solvent cast, (a) PLA, (b) PHA, and (c) CA.
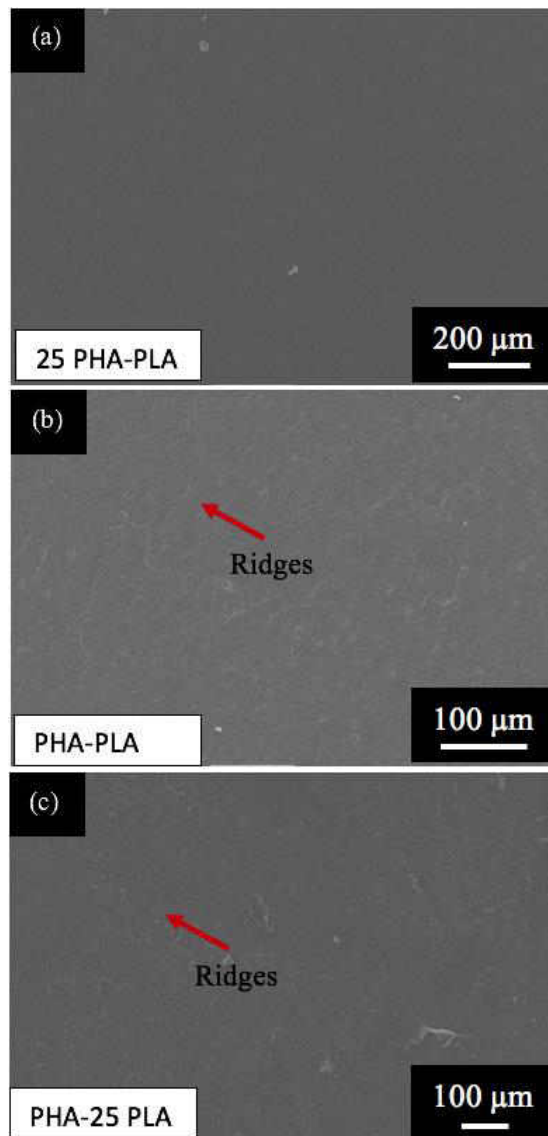
Figure 2.5: SE SEM micrographs of polished surface of blends of PLA-PHA fabricated by solvent casting, (a) 75 PLA – 25 PHA, (b) 50 PLA- 50 PHA, and (c) 25 PLA- 75 PHA.

Figures 2.6a and 2.6b show the microstructure of CA-PLA blend. Severe signs of demixing between CA and PLA were observed in 49 CA – 51 PLA (Fig. 2.6b) as compared to 24 CA – 76 PLA compositions (Fig. 2.6a). Digital pictures also showed severe demixing when CA content was increased in the PLA matrix (Figs. 2.6e-g). This observation indicates that the CA-PLA blend became unstable as the concentration of CA was increased in the PLA matrix. Comparatively, CA-PHA (Figs. 2.6 c-e) and 32 CA – 34 PHA – 34 PLA blends were uniform at the micron level (Fig. 2.6f).
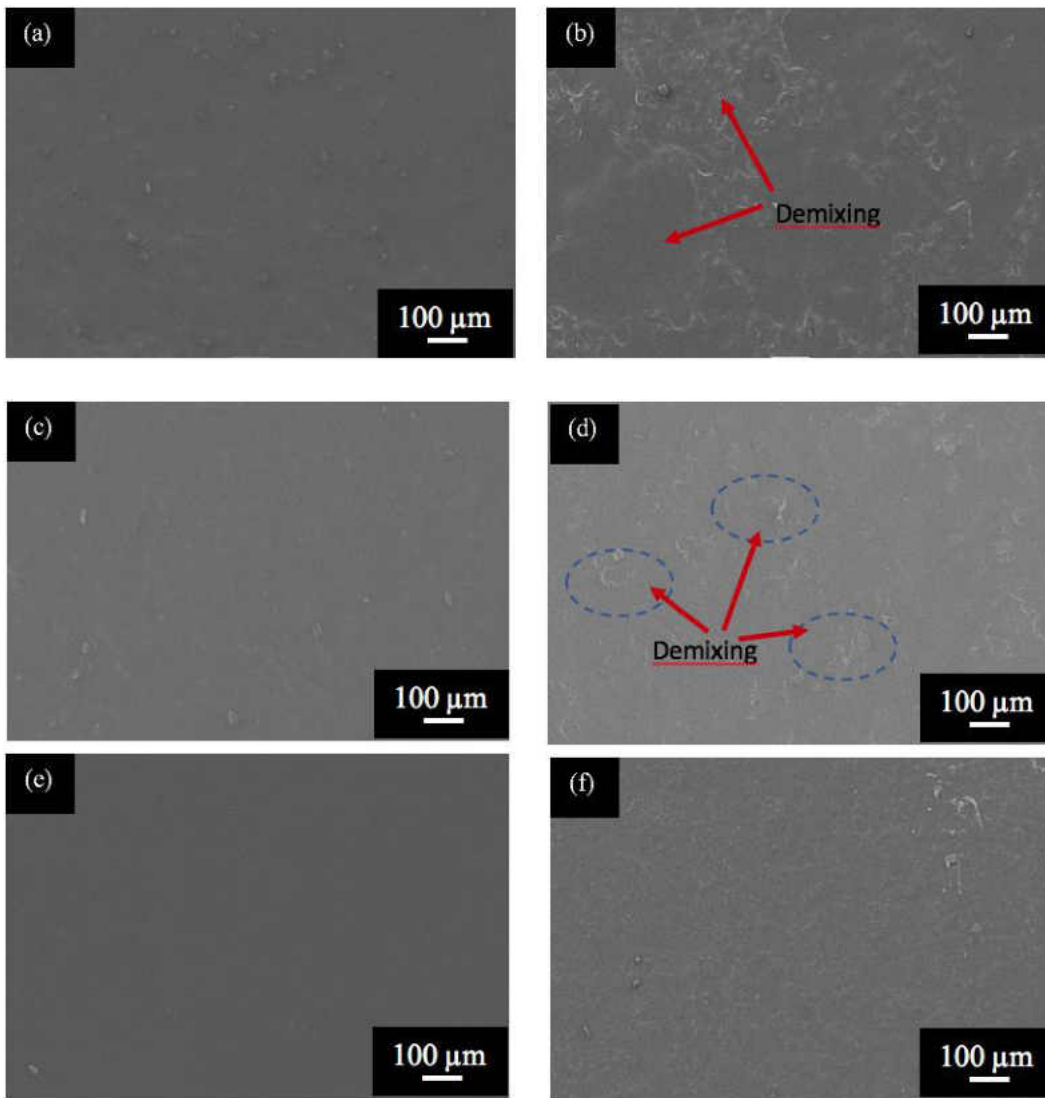
Figure 2.6: SE SEM micrographs of, (a) 24 CA – 76 PLA, (b) 49 CA – 51 PLA, (c) 49 CA – 51 PHA, (d) 74 CA – 26 PHA, (e) 90 CA – 10 PHA, and (f) 32 CA – 34 PHA – 34 PLA.

2.2.2 Summary of DSC Results

Figures 2.7a-b show the DSC results of PLA-PHA compositions. Table 2.3 summarizes the thermal characteristics of PHA-PLA blends. During first heating cycle, PLA showed semi-amorphous behavior and had a T_g (glass transition temperature) and T_m (melting point) of 65 and 144 ^{o}C, respectively. PHA showed two melting points (T_m and T_{m1}) at ~94 and ~152 ^{o}C. respectively. The 75 PLA - 25 PHA showed similar trend as PLA, T_g and T_m were observed at ~65 and ~147 ^{o}C, respectively. However, at higher volume content of PHA in PLA, for example in 50 PLA – 50 PHA, the blend showed characteristics of both PLA and PHA, and displayed T_g at 65 ^{o}C, and multiple melting points at 117 ^{o}C and 150 ^{o}C, respectively. Similarly, 25 PLA – 75 PHA showed multiple melting points at 112 ^{o}C and 153 ^{o}C, respectively, and T_g was observed at 60 ^{o}C.

During the second heating, PLA showed semi-amorphous behavior and had a T_g (glass transition temperature) and T_m (melting point) at 62 and 149 ^{o}C, respectively. On the other hand, PHA was predominantly crystalline, and T_c (crystallization temperature) and T_m were observed at 124 and 150 ^{o}C, respectively. The addition of PHA enhanced the T_c of PHA-PLA blend, and a predominant T_c was observed in 25 PLA – 75 PHA and 50 PHA – 50 PLA, thereafter the blends became semi-amorphous as higher concentration of PLA was added in the blend. This study shows that PHA is sensitive to thermal history as compared to PLA, and the addition of PHA in PLA promotes crystallization of the PHA-PLA blend.

PLA-PHA blends have attracted a lot of research due to the fact that both the end members are biodegradable bioplastics [17, 18, 21-24]. Blumm et al. [21] had reported that the crystallization behavior of PHA-PLA is dependent on the molecular weight, for example, low-molecular-weight PLA (M_n = 1759) was miscible over the entire range. Comparatively, blend of high-molecular-weight PLA (M_n = 159400) with PHB (poly(hydroxybutyrate - simple and

common representative of PHA) [17]) showed phase separation. Zhang et al. [22] studied blends of different PLA/PHB weight ratios of 100/0, 75/25, 50/50, 25/75, and 0/100 by melt compounding. They observed that both the polymers are immiscible over the entire range. Zhang et al. [22] also reported that PHB increased the crystallinity and heat distortion temperature of the PLA matrix and increased its heat distortion temperature. They also reported that PLA/PHB 75/25 blend had better tensile properties as compared to PLA as the PHB addition promoted crystallization, and PHB crystallites acted as reinforcements in the biphasic mixture. Burzic et al. [23] reported that the addition of 20 wt% PHA (weight average molecular weight of 237560 g/mol) in PLA matrix promoted the crystallization and improved the impact resistance of PLA matrix. Tri et al. [24] had also reported that the addition of PHB and talc can synergistically increase the crystallization of PLA matrix. Janigova et al. [25] had observed multiple melting points in PHB and had attributed it due to the chain scission of the polymer which was responsible for bimodal distribution of crystallite size. In this study, we also observed multiple melting points in PHA and PHA rich blends during the first heating cycle (Fig. 2.7a). In this study, the samples were fabricated by solvent casting where polymers were dissolved in an organic solvent. The solvent casting process may be responsible for creating PHA based blends with multiple melting points. During the second heating cycle (the polymer was reconditioned by melting and cooling in DSC), a crystallization peak (T_c) was observed in PHA and PHA-rich composition in the temperature range of 124-130 $_o$C (Table 2.3). By analyzing this result, we can conclude that PHA helped in increasing the crystallization of the PLA matrix like it was observed in previous studies [22-24] (Fig. 2.7b).

Figure 2.7: DSC plots of, (a) PLA-PHA blends (first heating cycle), (b) PLA-PHA blends (second heating cycle) and first heating cycle of, (c) CA-PHA, (d) CA-PLA, and (e) CA-PLA-PHA blends.

Figure 2.7 c shows the DSC results of CA-PHA blends during the first heating cycle. Table 2.4 summarizes the thermal characteristics of CA-based blends. As described above, PHA is a predominantly crystalline polymer (T_m – 152 $_oC$) whereas CA is an amorphous polymer with a glass transition temperature (T_{gCA}) and melting point (T_{mCA}) of ~196 and ~230 $_oC$, respectively. Another endotherm at 210 $_oC$ is also observed during DSC of CA which is consistent with the observations of different investigators who have observed similar trend [26]. The exact mechanism of multiple endotherms which resulted in multiple melting points is not clear at this juncture. After the addition 24 vol% CA in the PHA matrix, the thermal characteristics of both CA (T_{mCA} – 222 $_oC$) and PHA (T_m – 148 $_oC$) were observed. However, at intermediate concentrations, for example 49 CA – 51 PHA, multiple melting temperatures were observed at 102 and 150 $_oC$, and T_{mCA} at 227 $_oC$ was observed, respectively. At higher concentrations of CA addition in PHA, for example 74 CA – 26 PHA, the T_m further reduced to 143 $_oC$, and T_{mCA} at 227 $_oC$ were observed. Comparatively, 89.5 CA – 10.5 PHA composition had multiple T_m of 115 and 145 $_oC$, respectively and a T_{mCA} of 223 $_oC$. In literature, there are various examples of cellulose addition in PHA, but very limited research data is available on CA-PHA blends [27, 28]. Wu [27] fabricated CA-PHA

17

(0, 5, 10, 15, and 20 wt% CA in PHA matrix) composites by hot pressing. They also observed that

the addition of 20 wt% CA in PHA reduced the melting point from 136.1 oC to 132.3 oC. The

authors also reported that the lowering of melting point was responsible for better processability

of CA-PHA blends [27]. They also observed that CA and PHA interfaces showed poor adhesion

due to different hydrophilicities of the two polymers, and the hydrogen bonding between CA. The

microstructure images presented by these authors also showed uneven distribution of CA in PHA

matrix. In solvent cast samples, we did not observe severe demixing in 49 CA – 51 PHA (Fig.

2.6c) but some signs of uneven distribution between respective constituents were observed in 74

CA – 26 PHA (Fig. 2.6 d). More microstructural evidence will be presented, when we will discuss

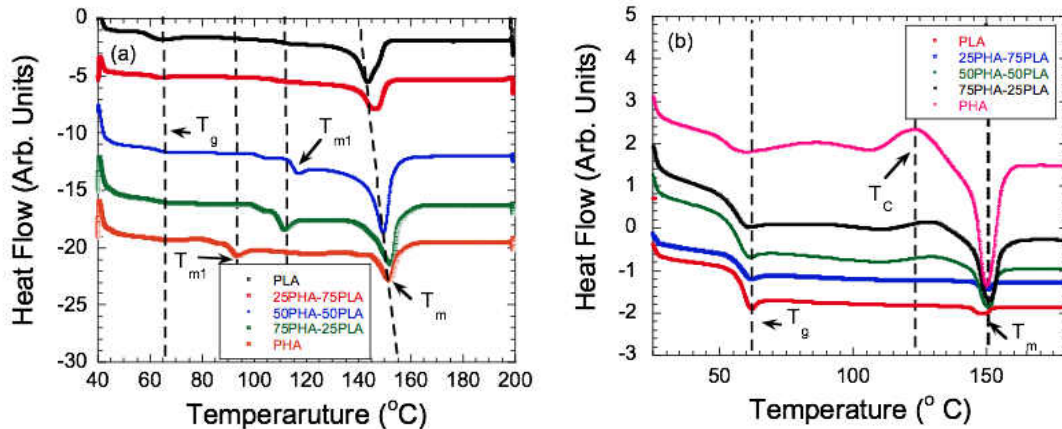the microstructure of the fractured surfaces in the section 2.2.4.

Figure 2.7: DSC plots of, (a) PLA-PHA blends (first heating cycle), (b) PLA-PHA blends
(second heating cycle) and first heating cycle of, (c) CA-PHA, (d) CA-PLA, and (e) CA-PLA-
PHA blends.

Further annealing studies are also needed to document whether demixing between CA and

PHA is enhanced by the heat treatment. Comparatively, Figure 2.7 d plots the DSC of 49 CA – 51

PLA which had a T_g and T_m (melting point) of 60 and 147 oC (similar to PLA Fig. 2.7a) and a

T_{mCA} at 229 oC like CA (Fig. 2.7d). This behavior indicates that PLA and CA are immiscible.

Wang et al. [29] also reported incompatibility between PLA and CA.

Figure 2.7e shows the thermal characteristics of CA-PHA-PLA blends. After the addition of 5 vol% CA in the PHA-PLA matrix, the T_g and T_{mCA} due to the presence of both CA and PLA constituents in blend was not detected in the DSC plot. Multiple T_m was also observed at 100 $_o$C and 149 $_o$C, respectively (Table 2.4). In addition, a shoulder peak (T_s) was also observed at 128 $_o$C (50 PHA- 50 PLA did not show this peak during the first heating cycle (Fig. 2.7a)). This peak is often observed in PLA and is attributed to the recrystallization to ordered α-crystal from loose and disordered chain α'-crystal form [23, 30]. PHA also showed similar crystallization temperature during the second heating cycle (Fig. 2.7b). The addition of 19 vol% CA in PHA-PLA matrix also showed similar characteristics as 5 vol% CA additions. From these observations, we can conclude that CA aids in the crystallization of PLA-PHA matrix after the additions of low concentrations of CA (≤ 19 vol%).
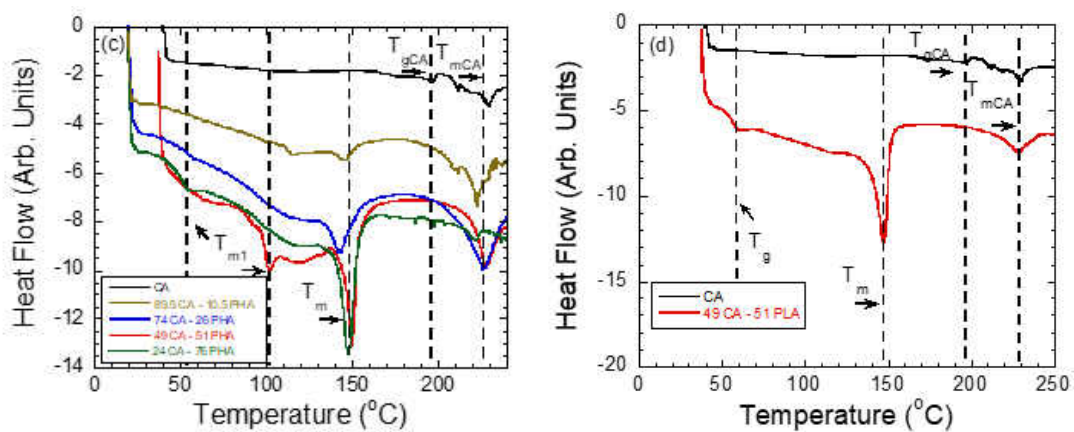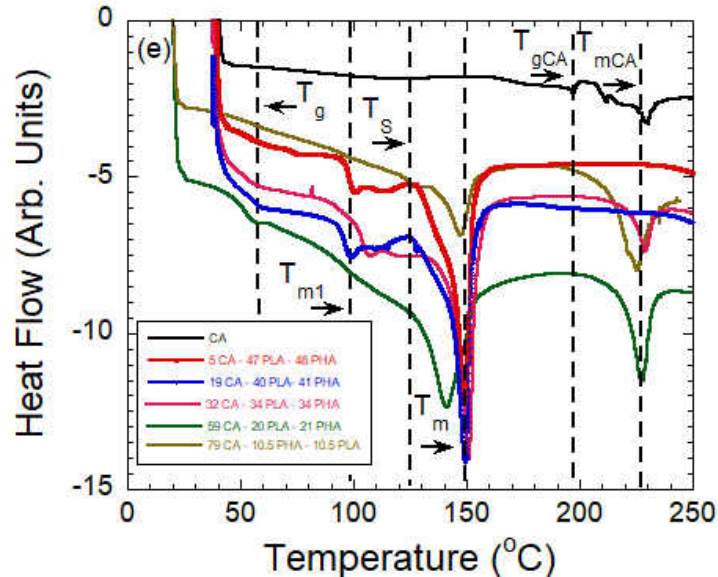

Figure 2.7: DSC plots of, (a) PLA-PHA blends (first heating cycle), (b) PLA-PHA blends (second heating cycle) and first heating cycle of, (c) CA-PHA, (d) CA-PLA, and (e) CA-PLA-PHA blends.

Table 2.3: Thermal characteristics of PHA-PLA blends

Composition (vol%)	Heating Cycle	T_g ($_oC$)	T_c ($_oC$)	T_{m1} ($_oC$)	T_m ($_oC$)
100 PLA		65		x	144
100 PHA		x		94	152
75 PLA – 25 PHA	1st	65	x	x	147
50 PLA - 50 PHA		65		117	150
25 PLA - 75 PHA		60		112	153
100 PLA		62	x		149
100 PHA		x	124		150
75 PLA – 25 PHA	2nd	62	x	x	150
50 PLA - 50 PHA		61	130		151
25 PLA - 75 PHA		61	130		151

The 32 CA – 34 PLA – 34 PHA blend showed multiple melting temperatures at 108 $_oC$ and 151 $_oC$, and the characteristic T_{mCA} peak due to CA constituent was observed at 229 $_oC$ (Table 2.4). 59 CA – 20 PLA – 21 PHA blend showed both T_g and T_m at lower temperatures of 57 $_oC$ and 141 $_oC$ as compared to T_g and T_m of 65 and 144 $_oC$, respectively for PLA (Table 2.3 and 2.4). In addition, the T_{mCA} at 228 $_oC$ was also observed in 59 CA – 20 PLA – 21 PHA which is a characteristic of CA component in the blend. Comparatively, 79 CA – 10.5 PLA – 10.5 PHA had T_m and T_{mCA} at 147 $_oC$ and 225 $_oC$, respectively. As a summary, the addition of higher amount of CA, for example 59 and 79 vol%, in PHA-PLA matrix increased the plasticity of the matrix which is further corroborated by lowering T_m of the blends.

Table 2.4: Thermal characteristics of CA-based blends

Composition (vol%)	T_g ($_o$C)	T_{gCA} ($_o$C)	T_S ($_o$C)	T_{m1} ($_o$C)	T_m ($_o$C)	T_{mCA} ($_o$C)
CA		196			x	210, 230
89.5 CA - 10.5 PHA				115	145	211, 223
74 CA - 26 PHA	x		x	x	143	227
49 CA - 51 PHA				102	150	227
24 CA - 76 PHA				57	148	222
49 CA - 51 PLA	60			x	147	229
5 CA - 47 PLA - 48 PHA	x	x	128	100	149	
19 CA – 40 PLA - 41 PHA	59		124	99	150	x
32 CA - 34 PLA - 34 PHA	58			108	151	229
59 CA - 20 PLA - 21 PHA	57		x	x	141	228
79 CA - 10.5 PLA - 10.5 PHA	x				147	225

2.2.3 Summary of Mechanical Behavior

Figure 2.8a shows the typical stress versus displacement plot of PLA, PHA, and different blends of PHA-PLA. PLA showed more plasticity and tensile strength as compared to PHA. Figure 2.8b summarizes the ultimate tensile strength of PLA, PHA, and their blends. PLA has a tensile strength of (59.4±8.19) MPa. The addition of PHA in the PLA matrix gradually reduced the tensile strength of the blend and reached its lower limit at PHA which had a tensile strength of (17.4±6.09) MPa. A mild enhancement of tensile strength in 50 PHA – 50 PLA was observed at (37.8±5.15) MPa as compared to 75 PLA – 25 PHA and 25 PLA – 75 PHA which had tensile strengths of (31.2±4.13) MPa and (22.9±7.78) MPa, respectively.

Zhang et al. [22] also reported that the additions of PHA in PLA in hot-pressed sample gradually reduced the strength of the PLA except PLA/PHB 75/25 which showed higher strength

than PLA due to the reinforcement of PLA matrix by crystallized PHB phase. Burzic et al. [23] observed that the addition of 10 and 20 wt% PHA in injection molded PLA reduced the tensile strength of the blends. They also reported that annealing for 1h at 100 ^{o}C improved the tensile strength of PLA/PHA3 (composite of 90% PLA with 10% PHA with a MW of 86958 g/mol) to 50 MPa which was comparable to the reported strength of annealed PLA. They attributed this behavior to the controlled crystallization of PHA in PLA matrix. By analyzing the literature and DSC results, the mild enhancement in tensile strength of 50 PHA – 50 PLA can be explained by the formation of PHA crystallites in PLA matrix. DSC results (Fig. 2.7a) also showed enhanced crystallization during the second heating cycles. It is also recommended that further annealing of PLA-PHA blends at higher temperatures can promote the crystallization of PHA in PLA matrix which can have a positive effect on mechanical strength.
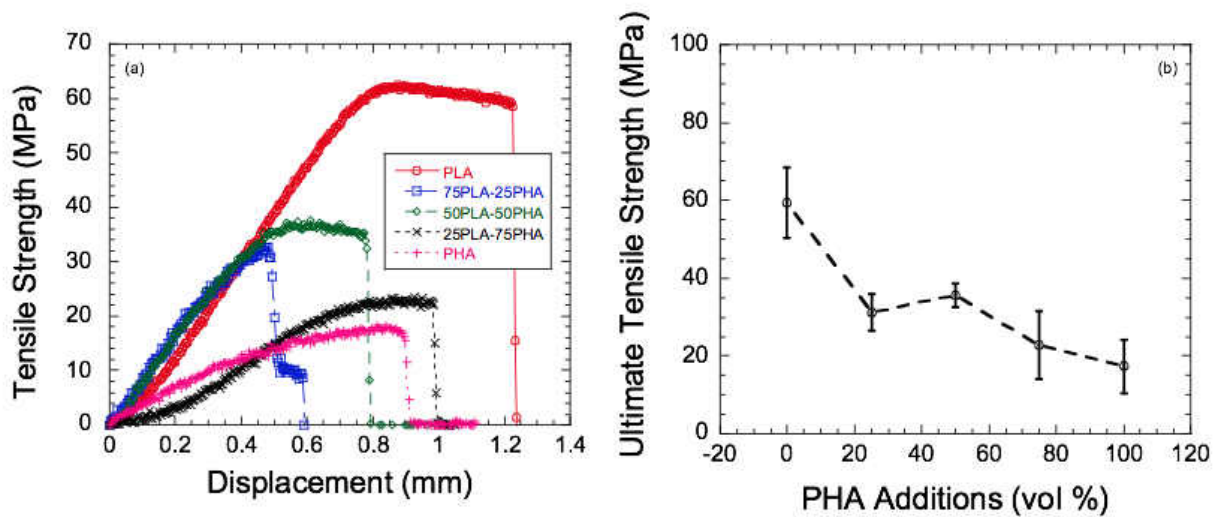

Figure 2.8: Plot of, (a) tensile stress versus displacement, and (b) UTS versus PHA additions in PLA-PHA blends.

Figure 2.9a shows the tensile stress versus displacement of CA-PHA blends. In general, both CA and PHA had lower tensile strength as compared to CA-PHA blends. Figure 2.9b summarizes the tensile strength of CA-PHA blends. PHA and CA had a tensile strength of

(17.4±6.82) MPa and (23.9±8.91) MPa, respectively. The addition of 24, 49,74, and 89.5 vol% CA in the PHA matrix improved the tensile strength to (25.8±1.06), (25.9±3.88) (44.9±3.41), and (42.4±5.01) MPa, respectively. By analyzing both the DSC and tensile strength results, it can be construed that the tensile strength of PHA can be improved by 1.5 times by adding controlled amount of CA in the PHA matrix (≤19 vol% CA). Comparatively, the tensile strength of CA can be improved by incorporating PHA in the CA matrix, for example the addition of 26% PHA in CA matrix enhanced the tensile strength by 1.9 times.

Based on earlier discussions of DSC results, it can be concluded that PHA and CA are immiscible. However, the addition of amorphous CA may have improved the plasticity of the blend which is also reflected by lowering of melting point of 74 CA – 26 PHA as compared to PHA (Table 2.4). In addition, PHA additions aided in the crystallization of the CA matrix. The synergistic effect of these two factors may have played an important role in increasing the strength of PHA-CA blends as compared to its end members. Wu [27] also reported that acrylic acid (AA) grafted PHA can further enhance the interaction between PHA and CA in hot pressed samples although the tensile strength of PHA (16.3 MPa) decreased after grafting with AA to 15.9 MPa. Wu [27] also reported that the addition of 20 wt% CA in the PHA matrix decreased the tensile strength to 7.8 MPa whereas the addition of 20 wt% CA in AA-PHA matrix increased the strength to 20 MPa. The author fabricated all the samples by hot pressing (exact details are not presented in the paper). Wu [27] also reported that CA and PHA phase separated in the composites (Fig. 3 in Ref. 27). Further studies are needed to understand whether processing conditions can further affect the immiscibility of PHA-CA matrix. Based on these results, it is also hypothesized that similar studies in solvent cast of CA-PHA blend by AA grafting can further enhance the tensile strength of these compositions.

Figure 2.9: Plot of, (a) tensile stress versus displacement, and (b) UTS versus CA additions in CA-PHA blends.

Figure 2.10a summarizes the tensile stress versus displacement plot. The tensile strength of PLA matrix detoriated from (59.4±8.19) MPa in PLA to (25.8±1.06) and (21.4±3.89) MPa after the additions of 24 and 49 vol% CA in PHA matrix, respectively (Fig. 2.10b). Wang et al. [29] also observed decrease in strength from ~ 44 MPa in PLA to ~20 MPa after the addition of 20 wt% CA in PLA matrix in hot pressed samples at 160 $_o$C. In CA-PLA system, hot pressed samples [29] are showing similar behavior as solvent cast samples due to the incompatibility between CA and PLA matrix.
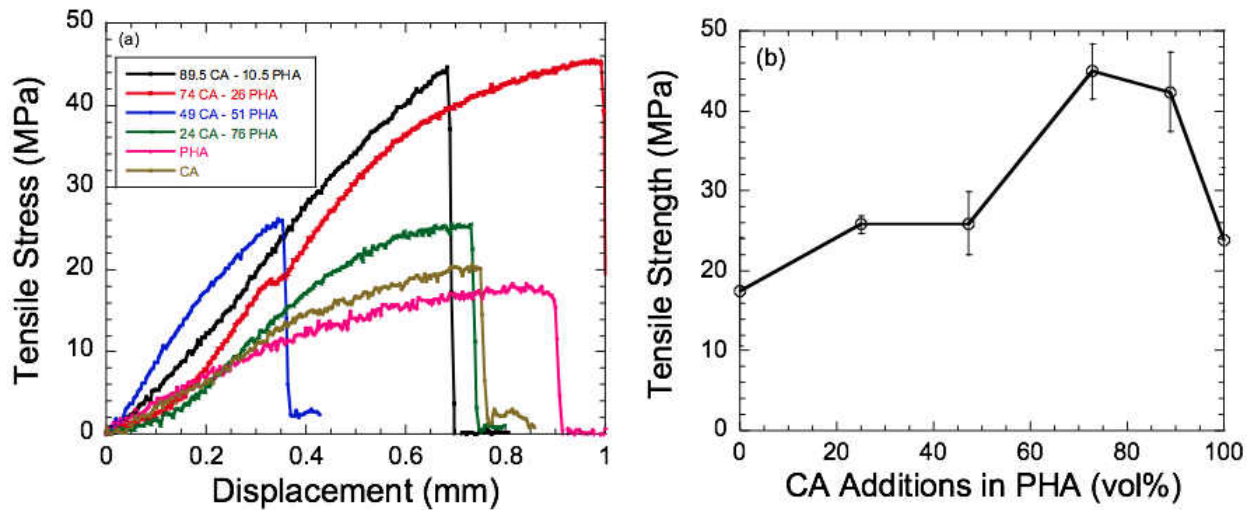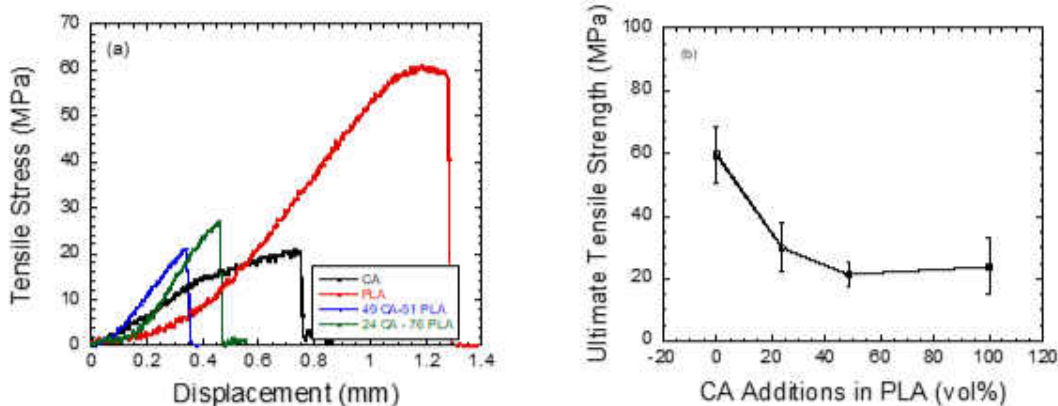
Figure 2.10: Plot of, (a) tensile stress versus displacement, and (b) UTS versus CA additions in CA-PLA blends.

Figure 2.11a plots the tensile stress versus displacement plots of CA-PHA-PLA blends where controlled amount of CA was gradually added in the PHA-PLA blends. For comparison, binary blend 50 PHA - 50 PLA had a tensile strength of (37.7±4.13) MPa as compared to (23.9±8.91) MPa in CA (Fig. 2.8b). The addition of 5 and 19 vol% CA degraded the strength of PHA-PLA to (22.6±9.08) and (21.8±4.33) MPa, respectively. The high crystallinity of these blends can account for the lower strength of these blends (Fig. 2.7e). It is possible that the addition of further lower amount of CA can control the crystallinity of PHA-PLA matrix and can enhance its strength.

However, after the addition of 32, 59, and 79 vol% CA in PHA-PLA matrix, the tensile strength improved to (32.9±1.66), (39.3±6.29), and (32.1±12.1) MPa, respectively. The increase in amorphous nature of the blend which is supported by the absence of T_s in 32 CA – 34 PLA – 34 PHA, 59 CA – 20 PLA – 21 PHA, and 79 CA - 10.5 PLA - 10.5 PHA (Table 2.4 and Fig. 2.7e) and mild lowering of T_m in these blends can explain the results. This study shows that the controlled additions of CA in PHA-PLA matrix can tailor the strength of PLA-PHA matrix, for example 59 CA – 20 PLA – 21 PHA has higher strength than 50 PHA- 50 PLA. This results clearly

25

indicates that CA-PHA-PLA system should be further explored as these blends can be solvent cast, and thus these blends can also act as feed for electrospinning.
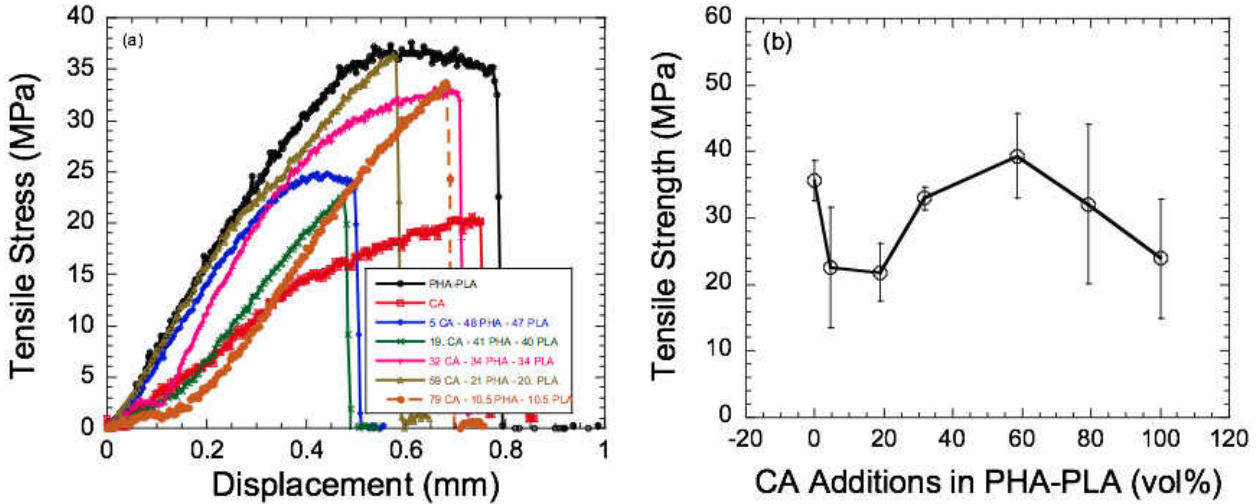
Figure 2.11: Plot of, (a) tensile stress versus displacement, and (b) UTS versus CA additions in PLA-PHA blends.

2.2.4 Analysis of Fractured Surface

Figure 2.12 shows the fractured surfaces of PLA, PHA, and CA samples. The fractured surface of PLA showed ligaments of PLA (> 10 µm) after tensile testing (Figs. 2.12a-b). The fractured surface of PHA showed the presence of micron-sized crystallites of PHA in the brittle PHA matrix (Figs. 2.12 c and d). Comparatively, CA also showed brittle fractured surface (Figs. 2.12 e and f).

Figures 2.13 a and b show the fractured surface of 50 PLA - 50 PHA composites like PLA fractured surface (Fig.2.12a), the fractured surface of 50 PLA - 50 PHA also showed the presence of finer polymer ligaments (≤ 5 µm) (Fig. 2.12 b). This result also further supports the hypothesis that the presence of crystalline PHA intertwined with PLA is responsible for lower plasticity and strength as compared to PLA matrix but higher strength than PHA blend (Fig. 2.8). The fractured surface of 24 CA – 76 PLA showed the phase separation of CA as micron-sized spherical globules

26

were observed in the PLA matrix (Figs. 2.13 c-d). Comparatively, 74 CA – 26 PHA (Figs. 2.13 e-f) did not show signs of phase separation like 24 CA – 76 PLA in the microscale although DSC results showed phase immiscibility between CA and PHA (Fig. 2.7 c). On further comparing the fractured surfaces of CA (Figs. 2.12 f) and 74 CA – 26 PHA (Fig. 2.13 f), finer polymer PHA crystallites can be observed in the CA matrix. This observation also provides evidence that PHA crystallites are reinforcing the CA matrix which is also potentially responsible for the 1.9 times enhancement in tensile strength of 74 CA – 26 PHA. Figures 2.13 g and h show the fractured surface of 59 CA - 20 PLA - 21 PHA. Unlike 24 CA – 76 PLA (Figs. 2.13 c-d), 59 CA - 20 PLA - 21 PHA showed a uniform fractured surface. Comparatively, the solvent cast 74 CA – 26 PLA blend was unstable and it separated into different constituents which were visible by naked eyes (Fig. 2.3g). From the presented evidence, we can conclude that PHA also helps in stabilizing CA-PLA blends.

Based on the current results, it can be summarized that PHA-PLA and CA-PHA binary blends showed promising results. Zhang et al. [22] had showed that optimized PLA/PHB 75/25 which showed higher strength than PLA due to the reinforcement of PLA matrix by crystallized PHB phase. Different investigators have added different types of additives like plasticizer (Lapol 108), nano-cellulose, limonene, and Poly(butylene succinate) in the binary blends to further engineer their properties [31-34]. The addition of 5 and 7 wt% Lapol 108 increased the plasticity but decreased the tensile strength of the PLA 75 – PHB 25 films which were fabricated by compression molding at 180 oC [31]. Arrieta et al. [32] used microextruder to fabricate plasticized PLA–PHB (75:25) blend with 15 wt% plasticizers (acetyl tributyl citrate (ATBC)), and 5 wt% cellulose nanocrystals (CNC) or modified cellulose nanocrystals with acid phosphate ester of ethoxylated nonylphenol (CNCs). The PLA–PHB–CNCs–ATBC blend showed better oxygen

barrier and stretchability. Due to immiscibility, PLA-PHB had multiple melting points at 149.6

and 172.7 oC whereas the addition of CNCs improved the interaction between PLA and PHB, and

PLA–PHB–CNCs–ATBC had a single melting point of 147.9 oC. They also reported that the

additions of CNCs improved the crystallinity of the blend. We also observed that the addition of 5

and 19 vol% CA improved the crystallinity of PLA-PHA blend although the tensile
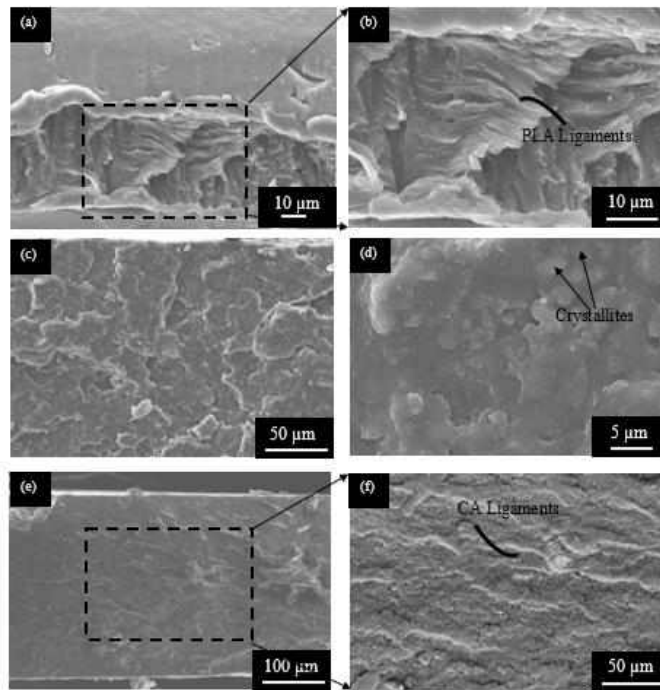
Figure 2.12: SEM SE micrographs of, (a) PLA, (b) PLA at higher magnification, (c) PHA, (d)
PHA at higher magnification, (e) CA, and (f) CA at higher magnification.
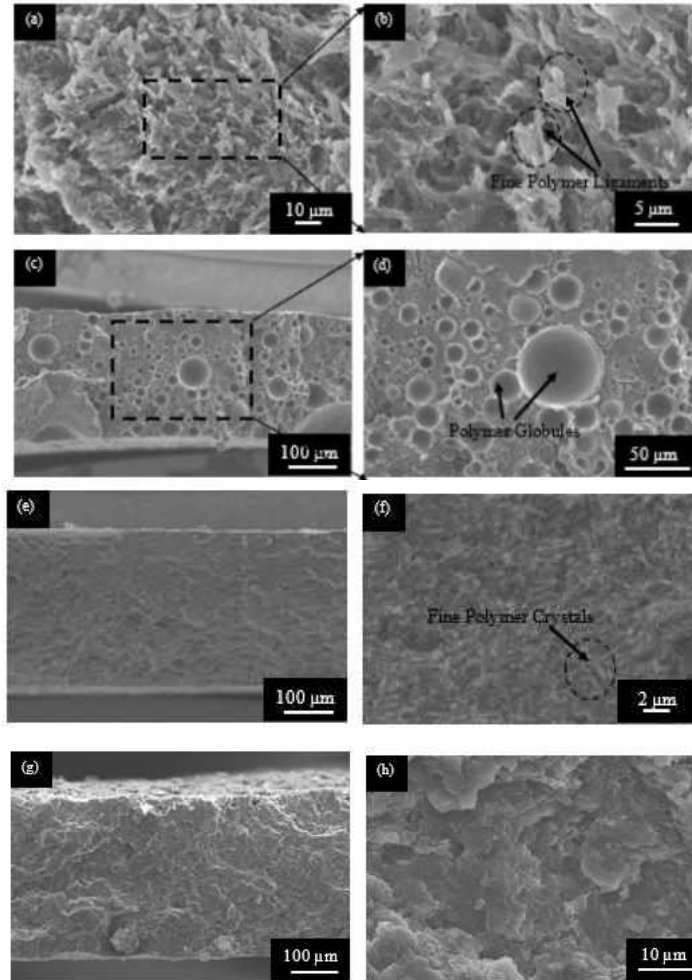
Figure 2.13: SEM SE micrographs of, (a) 50 PHA – 50 PLA, (b) PLA at higher magnification, (c) 24 CA – 76 PLA, (d) 24 CA – 76 PLA at higher magnification, (e) 74 CA - 26 PHA, (f) 74 CA - 26 PHA at higher magnification, (g) 59 CA - 20 PLA - 21 PHA, and (h) 59 CA - 20 PLA - 21 PHA at higher magnification.

strength of the blends was lower than PLA-PHA. It is recommended that these blends can be further engineered with plasticizers like Arrieta et al. [32]. However, at higher concentrations, CA was able to positively impact the tensile strength of the blend by increasing the plasticity of the ternary blends which was evident from the lowering of T_m in these blends (Table 2.4). In other words, ternary blend like CA-PLA-PHA gives us more engineering options for manufacturing sustainable and biodegradable composites. Furthermore, the addition of CA in the PHA-PLA

blend, or vice versa gives the design engineers an additional composition to designing blends for electrospinning as these blends are soluble in organic solvents.CA based blends also have the additional flexibility that these blends can converted back to cellulose by deacetylation [35].

2.3 Conclusion

Binary and ternary blends of PLA, PHA and CA were successfully fabricated by using solvent casting. DSC analysis showed that binary blends of PLA and PHA are immiscible in each other. By analyzing the second heating cycle, it was also construed that PHA is sensitive to thermal history as compared to PLA and promotes crystallization of PLA matrix. PLA has a tensile strength of (59.4±8.19) MPa. The addition of PHA in the PLA matrix gradually reduced the tensile strength of the blend and reached its lower limit at PHA which had a tensile strength of (17.4±6.09) MPa. Comparatively, a mild enhancement in strength in 50 PHA – 50 PLA was observed at (37.8±5.15) MPa as compared to 75 PLA – 25 PHA and 25 PLA – 75 PHA which had tensile strengths of (31.2±4.13) MPa and (22.9±7.78) MPa, respectively. This may be due to the formation of crystallized PHA in PLA matrix which is further supported by DSC results. This hypothesis was also supported by the inspection of fractured surface of 50 PHA – 50 PLA.

PHA and CA had a tensile strength of (17.4±6.82) MPa and (23.9±8.91) MPa, respectively. Comparatively, the addition of 24, 49,74, and 89.5 vol% CA in the PHA matrix improved the tensile strength to (25.8±1.06), (25.9±3.88) (44.9±3.41), and (42.4±5.01) MPa, respectively. This enhancement in strength can be explained by the synergistic effects of adding, (a) CA in PHA which improved plasticity of the blends, and (b) PHA in CA matrix which helped in reinforcing the CA matrix with PHA crystallites.

The addition of CA in PLA caused severe demixing, and the strength of PLA matrix detoriated from (59.4±8.19) MPa in PLA to (25.8±1.06) and (21.4±3.89) MPa after the additions

of 24 and 49 vol% CA in PHA matrix, respectively. The 74 CA - 26 PLA composition phase showed visible separation into agglomerates of different constituents hence it could not be tested for tensile strength.

Comparatively, binary blend 50 PHA - 50 PLA had a tensile strength of (37.7±4.13) MPa as compared to (23.9±8.91) MPa in CA. The addition of 5 and 19 vol% CA degraded the strength of PHA-PLA to (22.6±9.08) and (21.8±4.33) MPa, respectively. The DSC results showed that these blends are high crystalline which can explain the lower strength of these. However, after the addition of higher concentrations of CA, for example 32, 59, and 79 vol% CA additions in PHA-PLA matrix, the strength improved to (32.9±1.66), (39.3±6.29), and (32.1±12.1) MPa, respectively. The enhancement in strength can be explained by the increase in amorphous nature of these blend which was further supported by the absence of T_s in these blends from DSC results. This study shows that the controlled additions of CA in PHA-PLA matrix can tailor the strength of PHA-PLA matrix which renders ternary blends as valuable component for sustainability research.

CHAPTER III

SYNTHESIS AND CHARACTERIZATION OF NOVEL PHA-PLA COMPOSITES BY ADDITIVE MAFUCTURING TECHNIQUES

3.1 Introduction

3.1.1 Lignin

Lignin is among the most abundant natural polymers that are found in nature. The natural polymers are cellulose, lignin, and hemicellulose [36]. Lignin can be found in plants and it mainly acts as a rigidity provider to them so they can be protected from biological hazards such as bacteria and viruses [37]. Lignin is commercially available in the pulp and paper industry [38]. The process of isolating lignin from its source can be described in three steps, (a) cell wall is broken by ball milling, (b) solvent extraction of lignin, and (c) purification of lignin [39].

Lignin is a sustainable material bestowed with excellent properties like biocompatibility, biodegradability, and eco-friendly. Lignin integration with synthetic polymers such as polypropylene (PP) and poly(ethylene terephthalate) (PET) are widely reported in literature [40, 41]. It was reported that when lignin is added to PP, it acted as an effective processing stabilizer and a light stabiliser. However, the tensile strength of PP deteriorated when lignin content is in the matrix, even at low percentages [42]. PLA-lignin composites were also evaluated using the solvent casting technique. The acetylation of lignin enhanced the mechanical properties and heterogenous nucleation of the composites due to better compatibility and interface area between PLA and lignin [43].

In this chapter, the synthesis of novel PHA-PLA polymer matrix composites reinforced with lignin particulates will be reported. This study will further help in understanding the chemistry and mechanics of lignin interaction with polymer matrices. The thermal and the mechanical behaviors of these composites will be also reported in this chapter.

3.1.2 Silver (Ag)

Natural or ionic forms of silver compounds are used in a wide variety of applications including medical devices, home appliances, and water treatment. Nano-sized silver particles have applications in diverse fields like electronics, health care industry, food-packing and many more due to its high surface area [44].

Silver nanoparticles are also known for antibacterial properties against Gram positive and Gram negative bacteria in many biomedical and food packaging applications [45]. Polylactic Acid (PLA) is also known for its compatibility with variety of foods such as beverages, fresh meats, and dairy products [45]. PLA-Ag nanoparticles composites are manufactured by electrospinning technique and investigated in literature. It is reported that PLA nanofibers infiltrated with Ag-nanoparticles and Vitamin E have antibacterial and antioxidant characteristics [45].

In this study, the effect of micro-silver on the properties of PHA, PLA, and PHA-PLA matrices will be studied. The mechanical performance will be analyzed in this chapter.

3.2 Experimental Details

3.2.1 PHA-PLA-Lignin Composites

The detailed procedure for fabricating PHA-PLA composites by solvent casting is outlined in Chapter 2. PHA-PLA-Lignin composites were fabricated by the similar procedure. For example, 50wt%PHA-50wt%PLA samples with the addition of 9wt% of lignin (Indulin AT, MeadWestvaco, Richmond, VA) was fabricated by the following procedure. Initially, 2.275g of PHA and 2.275g of PLA were stirred with 50 ml of Dichloromethane for 1 h at room temperature. After that, 0.45g of as-received lignin powder was added to the mixture, and the entire slurry was stirred for an additional 1 h. Thereafter, 8g of the mixture was poured into a single compartment of Teflon coated pan. This resulted in 5 to 6 samples per mixture. Thereafter, the samples were cured at room temperature for 24 hours. The cured samples were cut into coupons for tensile testing

by a scissor. Finally, the samples were dried inside the furnace at 100 ₒC for 24 hours. Table 3.1

summarizes all the compositions fabricated during this study.

Table 3.1: List of fabricated samples for as-received lignin compositions

Composition (wt%)	PLA Content (g)	PHA Content (g)	As-Received Lignin Content (g)
50 PLA-50wt PHA-9% Lignin	2.275	2.275	0.45
50 PLA-50wt PHA-16% Lignin	2.1	2.1	0.8
50 PLA-50wt PHA-40% Lignin	1.5	1.5	2

3.2.2 Composites of PLA-PHA with Pyrolyzed Lignin AT 300 ₒC and 700 ₒC

Lignin powders were pyrolyzed at 300 ₒC and 700 ₒC in a tube furnace in flowing Argon

(Argon Tank, Praxair, Grand Forks, ND) environment for 1 h. The pyrolyzed powders were then

ball milled (8000 M mixer Mill, SPEX SamplePrep, Metuchen, NJ) for 10 minutes. After that, the

milled pyrolyzed lignin was crushed into fine powders by using a mortar and pestle. Thereafter,

the pyrolyzed lignin was sieved by -325 mesh sieve shaker (Gilson Performer III model: SS-3,

Gilson Company, Inc., Lewis Center, OH) for 1 h. PHA-PLA with pyrolyzed lignin composites

were then fabricated by using the procedure outline in the last section. Table 3.2 summarizes all

the composition synthesized during this study.

Table 3.2: List of fabricated samples for pyrolyzed lignin compositions at 300 ₒC

Composition (wt%)	PLA Content (g)	PHA Content (g)	Pyrolyzed Lignin Content (g)
50 PLA-50 PHA – 9% pyrolyzed lignin (300 ₒC)	2.275	2.275	0.45
50 PLA-50 PHA – 16% pyrolyzed lignin (300 ₒC)	2.1	2.1	0.8
50 PLA-50 PHA – 40% pyrolyzed lignin (300 ₒC)	1.5	1.5	2

Table 3.3: List of fabricated samples for pyrolyzed lignin compositions at 700 $_o$C

Composition	PLA Content (g)	PHA Content (g)	Pyrolyzed Lignin Content (g)
50 PLA-50 PHA–9% pyrolyzed lignin (700 $_o$C)	2.275	2.275	0.45
50 PLA-50 PHA – 16% pyrolyzed lignin (300 $_o$C)	2.1	2.1	0.8
50 PLA-50 PHA – 40% pyrolyzed lignin (700 $_o$C)	1.5	1.5	2

3.2.3 PHA, PLA, and PHA-PLA Micro-Silver Composites

Please refer to Chapter II regarding the fabrication procedure for PHA, PLA, and PHA-PLA composites. All micro-silver composites were fabricated by the similar procedure. PHA-1wt%Ag was prepared by dissolving 4.95 g PHA granules in 50 ml Dichloromethane by magnetically stirring process as discussed previously. After one hour of stirring, micro-silver (Silver powder, 2-3.5 µm, ≥ 99.9% trace metal basis, Sigma-Aldrich, St. Louis, MO) was added, then the slurry was stirred for an additional hour. Afterwards, the mixture was poured into a Teflon coated pan, each compartment contained 8g of the mixture. This resulted in 5 to 6 samples per mixture. Thereafter, the samples were cured at room temperature for 24 hours. Afterwards, the samples were machined for mechanical testing. Finally, the samples were put inside the furnace at 100 $_o$C for 24 hours. Table 3.4 summarizes all the compositions manufactured during this study.

Table 3.4: List of fabricated samples for micro-silver compositions

Composition (wt%)	PLA Content (g)	PHA Content (g)	Micro-Silver Content (g)
PHA-1wt%Ag	N/A	4.95	0.05
PLA-1wt%Ag	4.95	N/A	0.05
PLA-PHA-1wt%Ag	2.47	2.47	0.05

3.2.4 Mechanical Testing

All the samples were tested, and the data was analyzed by following the procedure outlined in Chapter II.
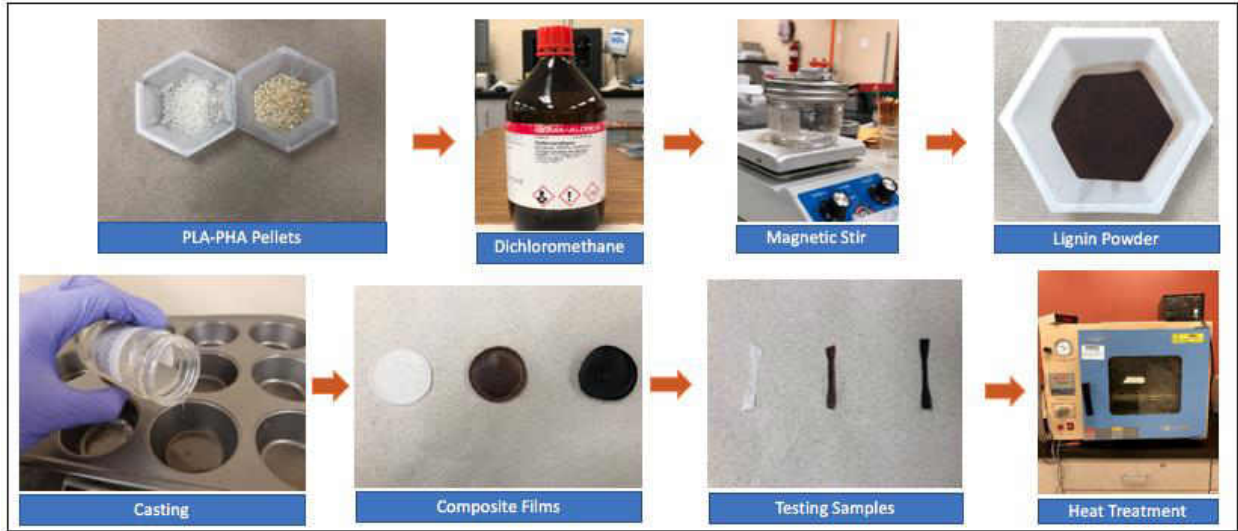
Figure 3.1: Fabrication procedure for as-received lignin composites.

3.3 Results and Discussions

3.3.1 Summary of Thermal Behavior of Lignin Composites

Figure 3.2 illustrates the thermal behavior of PHA-PLA-Lignin composites. In all the composites, T_m and T_g were 150 $_o$C and 60 $_o$C, respectively. These values are similar to the base PHA-PLA structure (Chapter II).
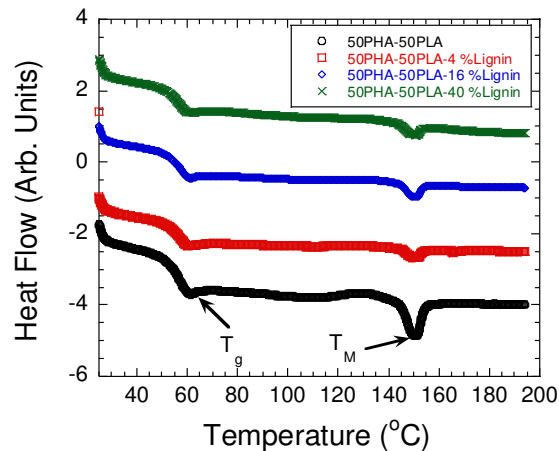

Figure 3.2: DSC plot of as-received lignin composites

3.3.2 Summary of Mechanical Behavior of Lignin Composites

Figure 3.3 shows the tensile strength versus the content addition of as-received and pyrolyzed lignin into PHA-PLA matrix. The tensile strength decreased as as-received or pyrolyzed lignin was added in the PHA-PLA matrix. After the addition of 9wt% and 16wt% pyrolyzed lignin at 300 oC and 700 oC, respectively, the tensile strength increased to (24.42±6.17) MPa and (20.26±2.14) MPa, and (24.81±6.60) MPa and (23.09±5.05) MPa respectively. Please note, 40wt% pyrolyzed lignin composites after pyrolysis at 300 oC and 700 oC were not analyzed due to their brittle nature. In addition, PHA-PLA composites with lignin pyrolyzed at 700 oC coiled during the drying process.

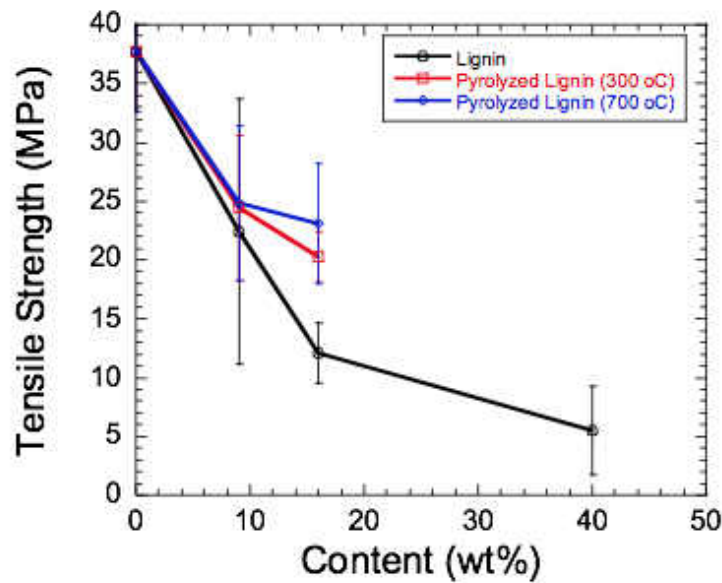Figure 3.3: Ultimate tensile strength versus lignin content in PHA-PLA matrix.

3.3.3 Summary of Mechanical Behavior of Micro-Silver Composites

Figure 3.4 compares the tensile strength of micro-silver composites with the base material. For instance, Figure 3.4a shows that the strength of PHA-1wt%Ag had higher tensile strength than PHA. Similarly, PLA-1wt% Ag had higher tensile strength than PLA (Fig. 3.4b). However, micro-

silver particles did not improve the tensile strength of PLA-PHA matrix. As reported in the previous chapter, the tensile strength of PLA-PHA matrix was (37.75±5.15) MPa, as compared to (34.16±4.74) MPa of PLA-PHA-1wt%Ag. Thus, it can be concluded that a very small amount of micro-silver particles, 1wt%, can enhance the tensile strength of PLA and PHA.
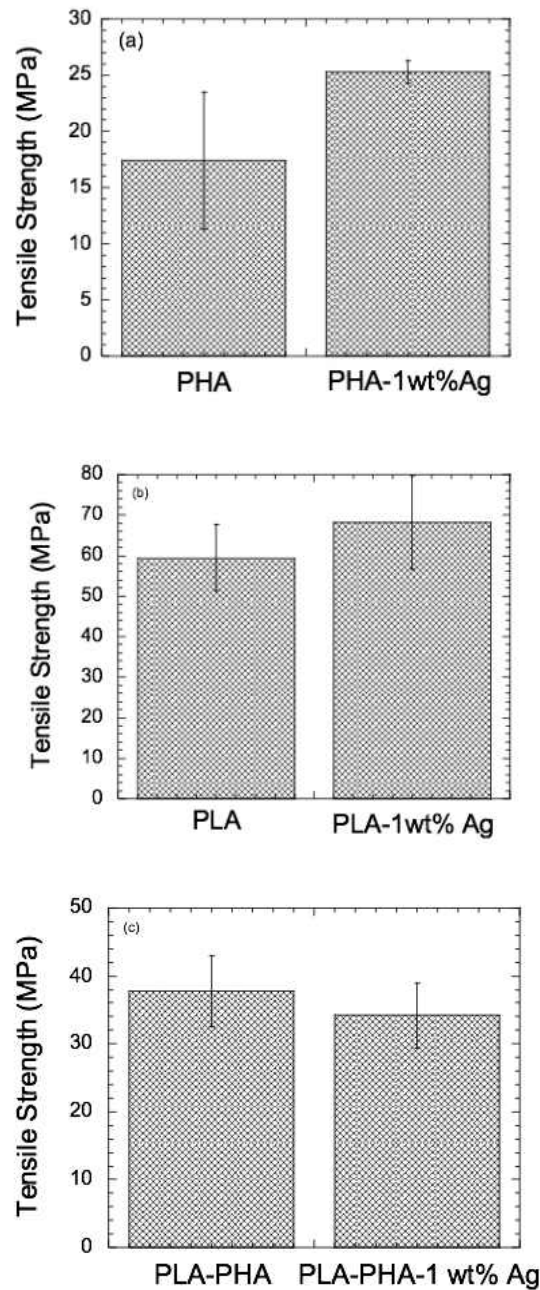

Figure 3.4: Plot of ultimate tensile strength of, (a) PHA and PHA-1wt%Ag, (b) PLA and PLA-1wt%Ag, and (c) PLA-PHA and PLA-PHA-1wt%Ag.

3.4 Conclusion and Future Work

PHA-PLA and lignin composites were successfully fabricated using the solvent casting technique. As-received lignin particles decreased the tensile strength of PHA-PLA matrix. However, pyrolyzed lignin at 300 $_o$C and 700 $_o$C showed a slight enhancement in the mechanical behavior as compared to the as-received lignin.

On the other hand, micro-silver particles were integrated into PHA, PLA, and PHA-PLA matrices, Micro-silver enhanced the tensile strength of PHA and PLA matrices. However, the strength has slightly decreased when micro-silver particles were incorporated into PHA-PLA matrix.

For future work, the thermal analysis of pyrolyzed lignin composites should be conducted to compare it to as-received lignin samples. This might help to investigate whether the pyrolysis of lignin would provide similar thermal stability to the material or not. Also, modifying the pyrolysis temperature such as 500 $_o$C and 900 $_o$C are recommended, as it could lead to better performance in the mechanical properties. Furthermore, bacteria activity study such as antimicrobial analysis is recommended, this is because of what was reported from literature review about silver, as it has antimicrobial properties. Cobalt is another candidate to be integrated to the polymers as it is also known for its antimicrobial characteristics.

APPENDIX

Status of Journal Publications

1. "On the Design of Novel PLA/PHA and Lignin-based Composites", S. Abu Aldam, M. Dey, S. Javid, Y. Ji, S. Gupta, Journal of Materials Engineering and Performance, (to be submitted), 2019

Contributed Presentations during Master's Degree

1. "On the Design of Novel PLA/PHA and Lignin-based Composites", S. Abu Aldam, M. Dey, S. Javid, Y. Ji, S. Gupta, Graduate Student Seminar, UND, 2019

2. "On the Design of Novel PLA/PHA and Lignin-based Composites", S. Abu Aldam, K. Hall, M. Dey, Y. Ji, S. Gupta, Materials Science and Technology Conference, Portland, Oregon, 2019

3. "On the Design of Novel PLA/PHA Composites", S. Abu Aldam, K. Hall, M. Dey, Y. Ji, S. Gupta, GRADay, UND, 2019

4. "On the Design of Novel PLA/PHA Composites", S. Abu Aldam, K. Hall, M. Dey, Y. Ji, S. Gupta, ND EPSCoR, Fargo, North Dakota, 2019

5. "On the Design of Novel Lignin-based Composites", S. Abu Aldam, M. Dey, K. Hall, Y. Ji, S. Gupta, ICACC 2019, Daytona Beach, Florida

REFERENCES

[1] "What is a circular economy", Ellen Macarthur Foundation, [Online], Available: https://www.ellenmacarthurfoundation.org/circular-economy/concept. Accessed November 5, 2019

[2] "New Plastics Economy", Ellen Macarthur Foundation, [Online], Available: https://www.ellenmacarthurfoundation.org/our-work/activities/new-plastics-economy. Accessed November 5, 2019

[3] "Rethinking the future of plastics", Ellen Macarthur Foundation, [Online], Available: https://www.newplasticseconomy.org/about/publications/report-2016. Accessed November 5, 2019

[4] "Lignocellulosics as sustainable resources for production of bioplastics - A review" Malin Brodin, María Vallejos, Mihaela Tanase Opedal, María Cristina Area, Gary Chinga-Carrasco, Journal of Cleaner Production **162,** 646-664 (2017).

[5] "Overview of Poly(Lactic Acid) (PLA) Fibre, Fibre Chemistry", Ozan Avinc, Akbar Khoddami, **41**, 68-78 (2009).

[6] "Physical and mechanical properties of PLA, and their functions in widespread applications – A comprehensive review", Shady Farah, Daniel G. Anderson, Robert Langer, Advanced Drug Delivery Reviews **107**, 367-392 (2016).

[7] "Polylactic Acid Technology", Ray E. Drumright, Patrick R. Gruber, and David E. Henton, Adv. Mater., **12**, 1841-46 (2000).

[8] "4043D Technical Data Sheet", https://www.natureworksllc.com/

[9] "Polyhydroxyalkanoates: an overview" C.S.K. Reddy, R. Ghai, Rashmi, V.C. Kalia, Bioresource Technology **87**, 137-146, (2003).

[10] "Producing PHAs in the bioeconomy – Towards a sustainable bioplastic", Karolin Dietrich, Marie-Josee Dumont, Luis F. Del Rio, Valerie Orsat, Sustainable Production and Consumption, Vol. **9**, January, pages 58-70, (2017).

[11] "Commercial application of cellulose nano-composites – A review" Amita Sharma, Manisha Thakur, Munna Bhattacharya, Tamal Mandal, Saswata Goswami, Biotechnology Reports xxx (2018) xxx–xxx.

[12] "Cellulose acetate electrospun nanofibers for drug delivery systems: Applications and recent advances", Kamyar Khoshnevisan, Hassan Maleki, Hadi Samadian, Shadab Shahsavari, Mohammad Hossein Sarrafzadeh, Bagher Larijani, Farid Abedin Dorkoosh, Vahid Haghpanah, Mohammad Reza Khorramizadeh, Carbohydrate Polymers **198,** 131–141(2018).

[13] "Properties and Applications of Cellulose Acetate", Steffen Fischer, Katrin Thummler, Bert Volkert, Kay Hettrich, Ingeborg Schmidit, Klaus Fischer, Macromol. Symp., **262**, 89-96, (2008).

[14] "Production, use, and fate of all plastics ever made", Roland Geyer, Jenna R. Jambeck, Kara Lavender Law, Sci. Adv. (2017);3: e1700782.

[15] "Bio-based and biodegradable plastics - Facts and Figures", Martien van den Oever, Karin Molenveld, Maarten van der Zee, Harriëtte Bos, Number Wageningen, Food & Biobased Research number 1722, ISBN-number 978-94-6343-121-7 DOI http://dx.doi.org/10.18174/408350 (2017).

[16] "Bio-Based and Biodegradable Plastics: An Assessment of the Value Chain for BioBased and Biodegradable Plastics in Norway", Norwegian Environment Agency, Project number – 1446 (2018).

[17] "On the Use of PLA-PHB Blends for Sustainable Food Packaging Applications", Marina Patricia Arrieta, María Dolores Samper, Miguel Aldas, and Juan López, Materials **10**, 1008; doi:10.3390/ma10091008 (2017).

[18] "Nanofiller Reinforced Biodegradable PLA/PHA Composites: Current Status and Future Trends", Jingyao Sun, Jingjing Shen, Shoukai Chen, Merideth A. Cooper, Hongbo Fu, Daming Wu, and Zhaogang Yang, Polymers **10**, 505; doi:10.3390/polym10050505 (2018).

[19] "Surface Functional Poly(lactic Acid) Electrospun Nanofibers for Biosensor Applications", Edurne González, Larissa M. Shepherd, Laura Saunders and Margaret W. Frey, Materials **9**, 47; doi:10.3390/ma9010047 (2016).

[20] "Analysis of the Degradation During Melt Processing of PLA/Biosilicate® Composites", Eduardo H. Backes, Laís de N. Pires, Lidiane C. Costa, Fabio R. Passador and Luiz A. Pessan, J. Compos. Sci. **3**, 52; doi:10.3390/jcs3020052 (2019).

[21] "Miscibility, crystallization and melting of poly(3=hydroxybutyrate)/poly(L-lactide) blends", E. Blumm and A. J. Owen, **36**, 4077-4081 (1995).

[22] "Blending Polylactic Acid with Polyhydroxybutyrate: The Effect on Thermal, Mechanical, and Biodegradation Properties", M. Zhang, N. L. Thomas, Advances in Polymer Technology, **30**, No. 2, 67–79 (2011).

[23] "Impact modification of PLA using biobased biodegradable PHA biopolymers", Ivana Burzic, Claudia Pretschuh, Dominik Kaineder, Gerhard Eder, Jiři Smilek,Jiři Masilko, Woss Kateryna, European Polymer Journal **114**, 32–38 (2019).

[24] "Crystallization behavior of poly(lactide)/poly(β-hydroxybutyrate)/talc composites", P.N. Tri, S. Domenek, A. Guinault, C. Sollogoub, J. Appl. Polym. Sci. **129**, 3355–3365 (2013).

[25] "Thermal degradation of plasticized poly(3-hydroxybutyrate) investigated by DSC", Ivica Janigova´, Igor Lacı´k, Ivan Choda´k, Polymer Degradation and Stability **77,** 35–41 (2002).

[26] "Characterization and Physical Properties of Cellulose Acetates", Peter Zugenmaier, Macromol. Symp. 2004, 208, 81-166.

[27] "Mechanical properties, biocompatibility, and biodegradation of cross-linked cellulose acetate-reinforced polyester composites", Chin-San Wu, Carbohydrate Polymers **105**, 41–48 (2014).

[28] "Green composites from sustainable cellulose nanofibrils: A review", H.P.S. Abdul Khalil , A.H. Bhat, A.F. Ireana Yusra, Carbohydrate Polymers **87**, 963– 979 (2012).

[29] "Polyester/Cellulose Acetate Composites: Preparation, Characterization and Biocompatible", Hui-Min Wang, Yi-Ting Chou, Chin-San Wu, Jen-Taut Yeh, Journal of Applied Polymer Science **126**, E242–E251 (2012).

[30] "Disorder-to-Order Phase Transition and Multiple Melting Behavior of Poly(L-lactide) Investigated by Simultaneous Measurements of WAXD and DSC", Jianming Zhang, Kohji Tashiro, Hideto Tsuji, Abraham J. Domb, Macromolecules, **41**, 1352-1357 (2008).

[31] "Thermal, mechanical and morphological characterization of plasticized PLA-PHB blends", Mohamed A. Abdelwahab, Allison Flynn, Bor-Sen Chiou, Syed Imam, William Orts, Emo Chiellini, Polymer Degradation and Stability **97**, 1822-1828 (2012).

[32] "Bionanocomposite films based on plasticized PLA–PHB/cellulose nanocrystal blends", M.P. Arrieta, E. Fortunati, F. Dominici, J. López, J.M. Kenny, Carbohydrate Polymers **121**, 265–275 (2015).

[33] "Ternary PLA–PHB–Limonene blends intended for biodegradable food packaging applications", Marina P. Arrieta, Juan López, Alberto Hernández, Emilio Rayón, European Polymer Journal **50**, 255–270 (2014).

[34] "Fully Biodegradable and Biorenewable Ternary Blends from Polylactide, Poly(3-hydroxybutyrate-co-hydroxyvalerate) and Poly(butylene succinate) with Balanced Properties", Kunyu Zhang, Amar K. Mohanty, and Manju Misra, ACS Appl. Mater. Interfaces **4**, 3091−3101 (2012).

[35] "Electrospinning of Ultrafine Cellulose Acetate Fibers: Studies of a New Solvent System and Deacetylation of Ultrafine Cellulose Acetate Fibers", W. K. Son, J. H. Youk, T S. Lee, W. H. Park, Journal of Polymer Science: Part B: Polymer Physics **42**, 5–11 (2004).

[36] "Lignin in straw of herbaceous crops", Anvar U. Buranov, G. Mazza, Industrial Crops and Products **28**, 237-259 (2008).

[37] Study of performance properties of lignin-based polyblends with polyvinyl chloride",Shivani B. Mishra, A.K. Mishra, N.K. Kaushik, Mukhtar A. Khan, "Journal of Materials Processing Technology, **183**, 273-276 (2007).

[38] Physicochemical properties of PLA lignin blends", Oihana Gordobil, Itziar Egues, Rodrigo Llano-Ponte, Jalel Labidi, "Polymer Degradation and Stability, **108**, 330-338, 2014.

[39] "Unmasking the structural features and properties of lignin from bamboo",Jia-Long Wen, Bai-Liang Xue, Feng Xu, Run-Cang Sun, Andre Pinkert, Industrial Crops and Products, 4**2**, 332-343, 2013.

[40] "Antioxidant properties of lignin in polypropylene",C. Pouteau, P. Dole, B. Cathala, L. Averous, N. Boquillon, Polymer Degradation and Stability, **81**, 9-18, 2003.

[41] "Supermolecular structure and thermal properties of poly(ethylene terephthalate)/lignin composites",M. Canetti, F. Bertini, Composites Science and Technology, **67**, 3151-3157, (2007).

[42] "The effect of blending lignin with polyethylene and polypropylene on physical properties", P. Alexy, B. Kosikkova, G. Podstranska, Polymer, **41**, 4901-4908, (2000).

[43] "All Biomas and UV Protection Composite Composed of Compatibilized Lignin and Poly (Lactic-acid)",Youngjum Kim, Jonghwan Suhr, Hee-Won Seo, Hanna Sun, Sanghoon Kim, In-Kyung Park, Soo-Hyun Kim, Youngkwan Lee, Kwang-Jin Kim, Jae-Do Nam, naturalsearch, March, 2017.

[44] "Polylactide (PLA)-based nanocomposites", Progress in Polymer Science, Jean-Marie Raquez, Youssef Habibi, Marius Murariu, Philippe Dubois, **38**, 1504-1542 (2013).

[45] "Polylactic acid (PLA)/Silver-NP/VitaminE bionanocomposite electrospun nanofibers with antibacterial and antioxidant activity", Bogdanel Silvetru Munteanu, Zeynep Aytac, Gina M. Pricope, Tamer Uyar, Cornelia Vasile, Journal of Nanoparticle Research, **16**, 2643, 2014.